MANSOURA JOURNAL OF Geology
Official Journal of Faculty of Science, Mansoura University, Egypt
E-mail: scimag@mans.edu.eg ISSN:

The detectability of the Cote d'Ivoire Infrasound Station (I17CI)

Hani. S. Elbehiri[a], Ibrahim Korrat[b] , Ahmed Lethy[a]*

[a]*National Research Institute of Astronomy and Geophysics (NRIAG), Egypt*

[b]*Geology Department, Faculty of Science, Mansoura University*

**** Correspondence to:** hany.saber@nriag.sci.eg*

Received:28/6/2022
Accepted: 24/7/2022

Abstract: Infrasound technology is one of the four techniques for the Comprehensive Nuclear-Test-Ban Treaty (CTBT) verification regime. The International Monitoring System (IMS) infrasound stations are established to monitor nuclear explosions in the atmosphere. This study aims to process and subsequently interpret the data obtained from the I17CI infrasound station situated at Cote d'Ivoire. The data is from 1st January 2013 until 20th April 2018. Progressive Multichannel Cross-Correlation (PMCC) algorithm with 11 different frequency bands is used for processing. Statistical analysis of the results noted 172,279 detections through the whole data set. The detections show seasonal and diurnal changes as they increase at night hours. At the night, detections are 110,480 representing 64.13% of all data. Comparing day- and night- hour detections indicate that most of them were recorded from continuous sources (microbaroms) recorded mainly at night hours. Microbaroms were detected at different azimuths extending from 105 to 360˚. From the Gulf of Guinea at azimuths between 105 and 200˚ that come from southwest Africa towards Atlantic Cold Tongue (ACT). Azimuths between 230 and 360˚ attributed to oceanic ones in front of Liberia, and azimuths between 320 and 340˚ from the ocean in front of Western Sahara. Other detections were recorded from other local sources to the east and thunderstorms from different directions.

keywords: Infrasound; Atmosphere; detections; Microbaroms

1.Introduction

An infrasound wave is a low-frequency sound wave with frequencies lower than the bottom limit of human audibility, ranging from 0.003 to 20 Hz [1]. Its propagation is strongly dependent on the atmosphere's temperature and wind structure [2]. It travels from its source through the atmosphere with ~ 343 m/s at 20° C [3], [4].These waves can travel thousands of kilometers through the atmosphere without considerable attenuation. Infrasonic waves are produced by a large number of natural and man-made sources. Natural sources include; volcanoes, meteorites, large earthquakes, thunderstorms, microbaroms, and avalanches. Man-made sources include; mining and chemical blasts, nuclear explosions, wind turbines, drones, helicopters, and rocket launches [5]–[7]. The (IMS) is a part of the CTBT verification regime [8], [9]. The IMS stations with their four categories; seismic, infrasound, hydro-acoustic, and radionuclide monitor the world for any nuclear explosion worldwide in the solid earth, atmosphere, and oceans. Currently, the IMS infrasound network Fig. (1) Contains 53 certified stations out of 60 planned to be constructed. These stations are distributed to detect, at least two stations any explosions in the atmosphere with a yield equivalent to 1 kiloton of TNT [10]. Studying the infrasound station detectability requires data analysis for a relatively long time.

2. Materials and methods

The study data are from the IMS infrasound I17CI station during the period 2013 to 21 April 2018. This station is in Cote d'Ivoire at a latitude 6.67° N and longitude -4.85° W Fig. (1) In a rural zone with a low-population density and relatively flat area. The environment surrounding it is rich in savannah for noise reduction. It consists of 4 elements of

DASE MB2000 which Commissariat à l'Energie Atomique develops (CEA) (French Atomic Energy Commission).

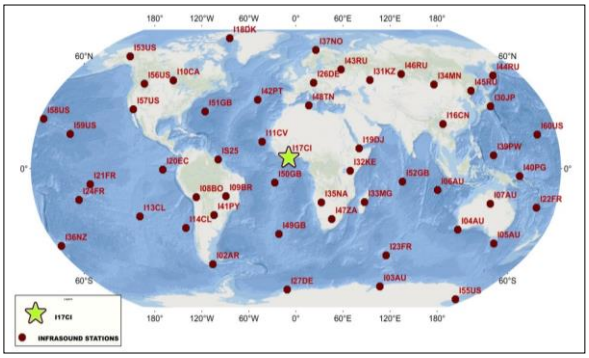

Fig. (1): The IMS infrasound network and the I17CI station.

The station data availability is almost above 98.11% at each year, and attains 99.58% during the study period Fig. (2) This indicates that the data is almost complete and continuous expect for a few maintenance hours each year.

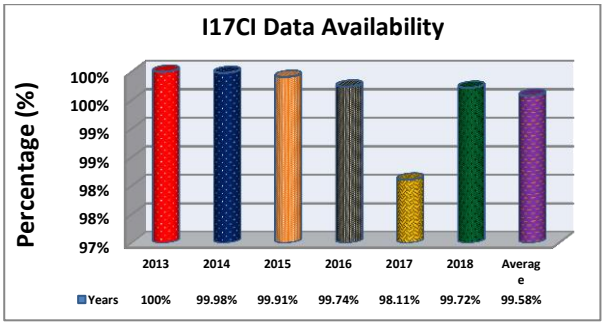

Fig. (2): Data availability at I17CI station.

The infrasound data processing approach is based on the Progressive Multichannel Cross-Correlation (PMCC) algorithm [11]–[13]. PMCC algorithm is used to cross-correlate and detects the delay time difference between arrivals at different elements. Detection theory supposes an array of 3 elements distributed at i, j, k and a plane wave moving through this array. There will be time delays in the wave arrival between every two elements. The delay between two sensors is symbolled by Δt. According to the closure relation, in case of neglecting the background noise, the sum of the delays in detection between every two elements should be zero.

$$\Delta tij + \Delta tjk + \Delta tki = 0$$

If there is a background noise within the wave propagating through the array elements, the accuracy of the cross-correlation operation decreases and the sum of delays between elements isn't exactly zero. The algorithm is progressively applied and the consistency value is calculated from the following relation.

$$Cn = \sqrt{\frac{6}{n\,(n-1)(n-2)}\, r_{ijk}^2}$$

Cn is the consistency value, n is the number of elements, and r_{ijk} is the sum of delays between elements i, j, and k are belongs to the array (R_n). The consistency value is calculated firstly from the delays between the smallest sub-elements triangle. The detection is stated if the consistency value is below the threshold used in processing [14]. Then the other elements are used to produce new sub-elements. Finally, the inversion algorithm calculates the azimuth and velocity values from the measured consistency values [15]. The PMCC algorithm uses 11 frequency bands in the data processing. These bands start from a very low frequency of 0.07 Hz and end at 4 Hz. The I17CI station detected a large number of detections throughout the whole data duration.

3. Results and Discussion

Using the PMCC algorithm a total of 172,279 detections with different azimuths detected; in the frequency range of 0.01 to 5 Hz were studied during the study period Fig. (3) Results in this figure are shown as a function of the calculated back-azimuth for a period from January 2013 to April 2018. Each dot indicates coherent infrasonic waves, with the color referring to the dominant frequency of the detected signals. The detections- scattering represents the detection density with time and azimuth.

The detections are distributed over time with different azimuths and frequencies. The distribution with azimuth is represented as a histogram of the detection's azimuth Fig. (4) Detections are mainly concentrated in three directions; large numbers in azimuths between 300- 360˚, 240-270˚ and ~ 110-150˚; which nearly correspond to N-NW, W, and SE directions.

Fig. (5) shows a histogram of the number of hourly detections during the 24-day hours. Fig. (6) Shows the day- and night-hours detections throughout the year. The daylight hours are almost 12 hours from 6 AM to 6 PM. The detections during daylight time are considered daytime detections. The night-hours detections

are much higher than day-hours detections. The day-hours detections are 61,799 constituting 35.87% of whole detections.

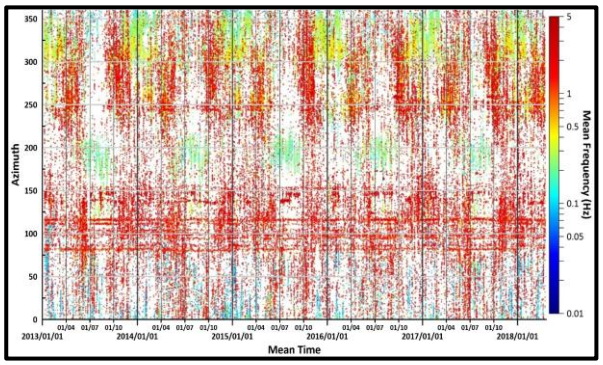

Fig. (3): Infrasound detections at I17CI station using the PMCC algorithm.

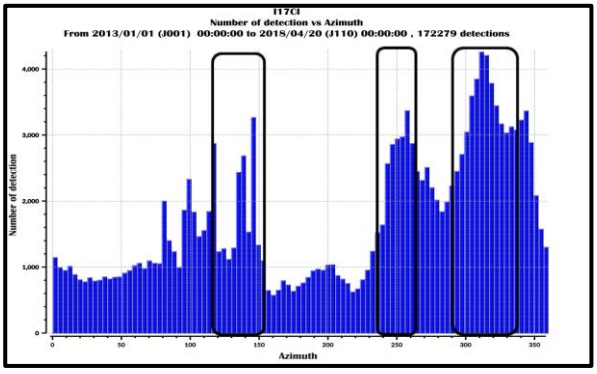

Fig. (4): I17CI station azimuthal-distribution detections.

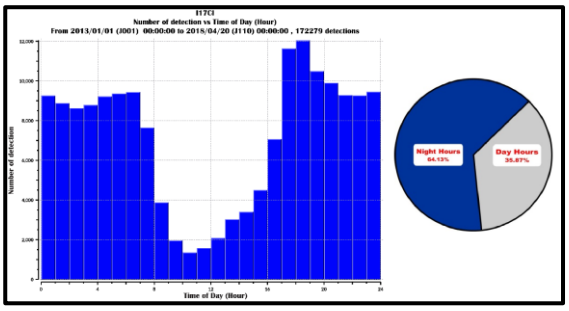

Fig. (5): Comparison of detection numbers between day and night hours.

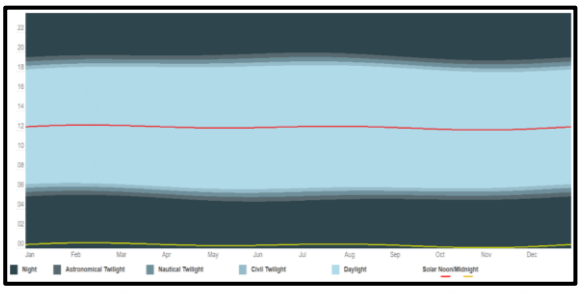

Fig. (6): The day/night hours throughout the year. The solar noon and midnight are indicated by red and yellow lines respectively.

The infrasound wave propagation is largely dependent on the wind and temperature profiles. The wave propagates in the atmosphere and is considered a moving medium, and the infrasound waves travel with the effective velocity [16] which depends on the wind speed and direction.

The meteorological data from five weather stations are used to study the effect of seasonal wind direction on infrasound detectability at the study station. Bouaké Airport, Yamoussoukro, Toumodi, Dimbokro Airport, and Tiassalé weather stations lie at 121, 51, 22, 23, 85 km from the I17CI station, respectively Fig. (7). The daily of the high- and low-temperatures in the five stations are presented in Fig. (8). The maximum-high temperature is 36 °C at Dimbokro station during February, and the minimum-high temperature is 27 °C at Bouaké station during August. The maximum-low temperature is 25 °C at Tiassalé station during March, and the minimum-low temperature is 19 °C at Yamoussoukro station during January. The climate at Côte d'Ivoire is generally tropical with a hot season lasting from November 22 to May 13, with an average daily high temperature $\geq 31°C$. The warm, rainy season lasts from July 3 to September 19, with an average daily high temperature $\leq 31°C$.

Wind direction is also a vital parameter that may affect infrasound detections. In general, the repetitive cycle of infrasound waves can give a reverse indication of the zonal wind. The maximum wind speed is about 12.24 km/h during August and the minimum wind speed is 6.84 km/h in November Fig. (9). About 75 % of the wind is from the south and southwest directions. The average wind direction percentage during the study period is listed in Table (1).

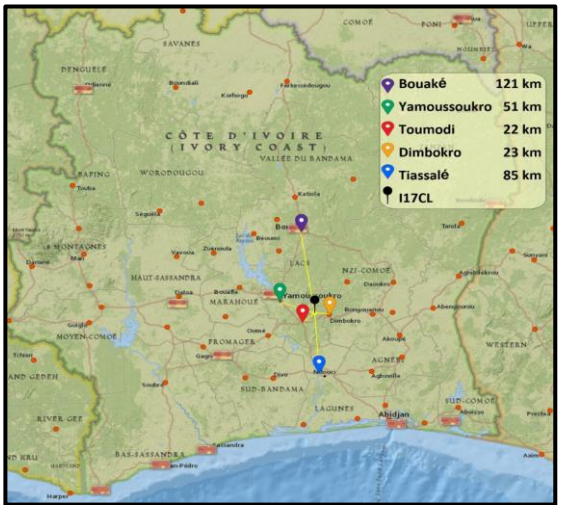

Fig. (7): The weather stations around the I17CI infrasound station.

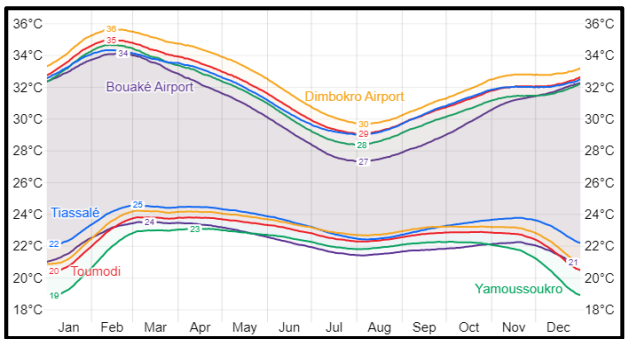

Fig. (8): The daily average high- and low-temperature in Bouaké Airport, Yamoussoukro, Toumodi, Dimbokro Airport, and Tiassalé weather stations in Côte d'Ivoire throughout the

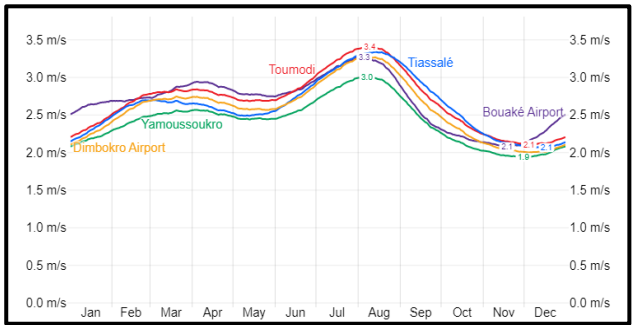

Figure 9: The daily average wind speed in Bouaké Airport, Yamoussoukro, Toumodi, Dimbokro Airport, and Tiassalé weather stations in Côte d'Ivoire throughout the year.

The dominant wind direction is that from the southwest with its maximum speed during the summer months (June to August). Almost small percentage of wind blows from the northwest and only about 11% from the west direction. However, most of detections are observed from the zone between the north and west directions. Meanwhile, a few detections are observed with the southward azimuth.

Table (1): Wind-direction (January 2013 - April 2018) [18].

Direction	Percent (%)
N	5 %
NE	3 %
E	2 %
SE	1 %
S	26 %
SW	49 %
W	11 %
NW	2 %

Initially, the detections at the study station are attributed to different sources such as thunderstorms and local events with frequencies up to 5 Hz from different back-azimuths. In addition to microbaroms detected from oceanic waves specifically the Atlantic Ocean. Some of these sources are detected seasonally and others continuously.

The data are split into sets to investigate the incompatible relationship between the source azimuth density distribution and the wind direction. The first is from 0.01 to < 0.5 Hz Fig. (10) which contains low-frequency detections from sources such as the microbaroms. The second set is from 0.5 to 5 Hz Fig. (11) Which contains high-frequency detections from sources such as thunderstorms and local artificial sources (explosions or jet planes).

Detections with frequency less than 0.5 Hz are mainly microbaroms Fig. (12) Which are distributed in various azimuths; especially from the southeast between 105-140˚, from the south 160-220˚, and from the west extending to northwest 230-350˚. These microbaroms detections are from the Atlantic Ocean surrounding the Côte d'Ivoire station, from northeast to south directions, and from the southeast at the Gulf of Guinea.

The detections between 105-140˚ show seasonal variations as it appears almost in summer from mid-May to the end of August Fig. (10). Also, detections from the south between azimuths 160-220˚ witness seasonal increase in warm season; spring and summer months from mid-April to the end of September Fig. (10). On the other hand, in the dry-hot season; from mid-November to mid-May, witness the microbaroms detections that come from the west and the northwest (between 230-350˚) Fig. (10).

However, frequency content between 0.5 to 5 Hz detections shows three clusters. The first has continuous detections all over the year near azimuth 100˚; from 80 to 120˚ Fig. (11). the second cluster is around azimuth ~150˚ with two occurrence periods from June to October and from December to the end of February. Finally, the detections from the west and northwest with azimuths between 220 and 350˚ have also two occurrence periods; between March and mid-June and September to end-November.

The infrasound detections are seasonally dependent; with single-cycle per year for those with frequency content less than 0.5 Hz, and two cycles per year for the higher frequency

ones. The detections periods and frequency of their seasonal occurrence are illustrated in Table (2).

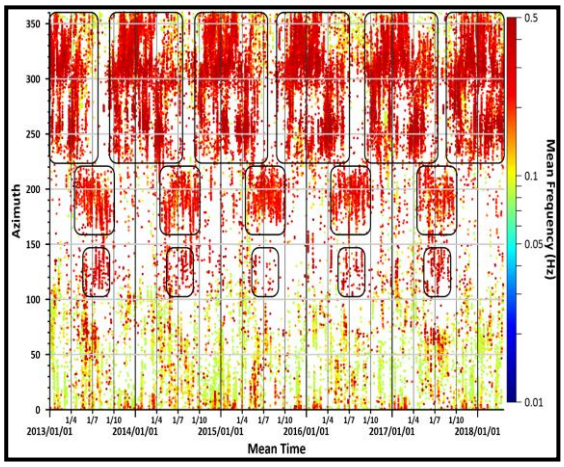

Fig. (10): Scattering of detection of frequency less than 0.5 Hz at I17CI. A total of 80,181 detections are included.

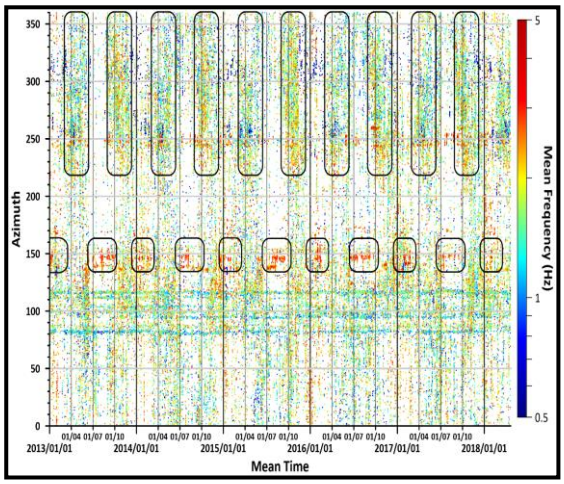

Fig. (11): Scattering of detections with frequency between 0.5 to 5 Hz at I17CI. A total of 92,097 detections are included.

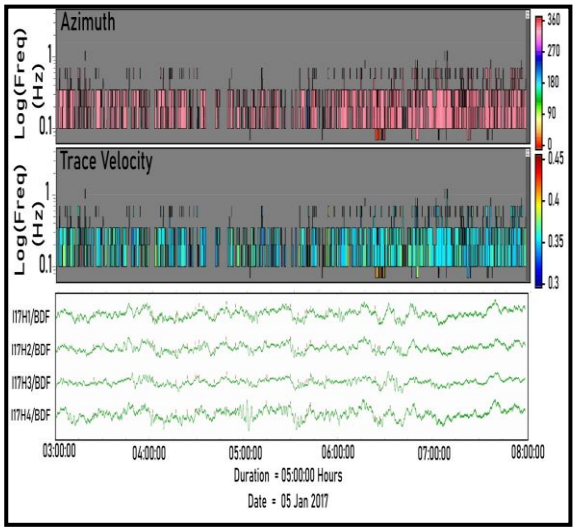

Fig. (12): Example of microbaroms detections at the I17CI station.

Table (2): The infrasound sources classification, with the dominant detection season at I17CI station.

Azimuth (˚)	Frequency (Hz)	Source	Months of year
105 - 140˚	Less 0.5 Hz	Microbaroms	mid-May to the end of August
	Above 0.5 Hz	Local events and thunderstorms	Continuous (All year)
160– 220˚	Less 0.5 Hz	Microbaroms	mid-April to the end of September
	Above 0.5 Hz	Local events and thunderstorms	between June to October, and November to February
230– 350˚	Less 0.5 Hz	Microbaroms	mid-September to the end of July
	Above 0.5 Hz	Local events and thunderstorms	March and mid-June and September to the end of November.

Fig. (12) Shows the back-azimuth of the detections polar-plotted on satellite image. Each column in the map represents the number of detections in this direction. Generally, the large number matches with microbaroms detections. Microbaroms are mainly concentrated in three azimuths directions; between 150-200˚, approximately near 200˚, and between 250-350˚. The largest detection number is in the bearing of the North Atlantic Ocean, specifically at azimuth 310˚. Otherwise, the longest bar represents it with a total number of 3,691 detections through the whole study period.

On the other hand, the minimum detection number is from the south, which is the dominant wind direction. This is because the detections-distribution of the microbaroms follows the hurricanes distribution in the Atlantic Ocean Fig. (13). Hurricanes in the South Atlantic Ocean are very rare. The lack of tropical cyclones in the South Atlantic Ocean is generally attributed to cool sea-surface temperatures and strong vertical wind shear. However [19] found 63 subtropical cyclones in the South Atlantic through the period from

1957 to 2007. Therefore, the microbaroms sources in the

south are less than their sources in the east and northeast directions.

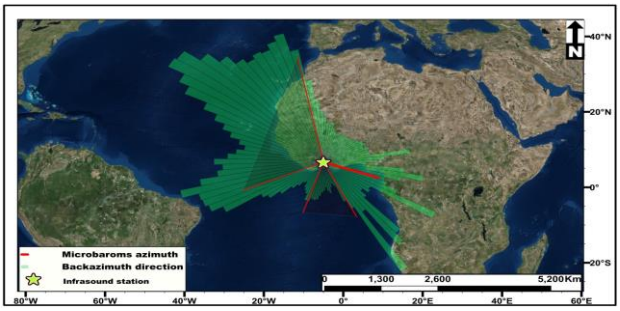

Fig. (12): Azimuth directions for detections and microbaroms sources.

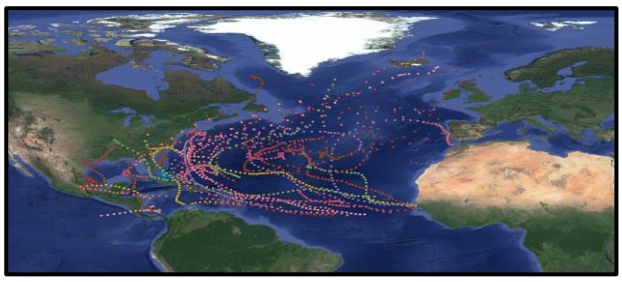

Fig. (13): Tracks of Atlantic tropical cyclones during the period 2013 to 2018.

In conclusion, the I17CI station is located in the western part of Africa where different sources of infrasound waves were detected. Sources such as thunderstorms and local activities are common but the main dominant source affecting this station is the continuous ocean surface oscillations (microbaroms). Detections at this station have both diurnal and seasonal variability. They have a higher probability at night hours than during day hours. Microbaroms are detected at 3 main azimuth zones; from 105 to 140˚, from 160 to 220˚, and between 230 and 350˚. This source classification is in agreement with the previous studies [20], [21].

The infrasound detections are seasonally dependent with single-cycle per year for those with frequency content less than 0.5 Hz which are mainly microbaroms, and two cycles per year for the high-frequency ones.

4. References

1 K. Kyriakides and H. G. Leventhall, (1977) "Some effects of infrasound on task performance," *J. Sound Vib.*, vol. **50**, no. 3, pp. 369–388, , doi: 10.1016/0022-460X(77)90490-4.

2 T. M. Georges, W. H. Beasley, T. M. Georges, and W. H. Beasley, (1977) "Refraction of infrasound by upper-atmospheric winds," *ASAJ*, vol. **61**, no. 1, pp. 28–34, doi: 10.1121/1.381263.

3 L. G. Evers and H. W. Haak, (2009), "The characteristics of infrasound, its propagation and some early history," *Infrasound Monit. Atmos. Stud.*, pp. 3–27, doi: 10.1007/978-1-4020-9508-5_1.

4 M. N. ElGabry, I. M. Korrat, H. M. Hussein, and I. H. Hamama, (2017) "Infrasound detection of meteors," *NRIAG J. Astron. Geophys.*, vol. **6**, no. 1, pp. 68–80, Jun., doi: 10.1016/J.NRJAG.2017.04.004.

5 P. Campus and D. R. Christie, (2010), "Worldwide observations of infrasonic waves," *Infrasound Monit. Atmos. Stud.*, pp. 185–234, doi: 10.1007/978-1-4020-9508-5_6.

6 J. Park, S. J. Arrowsmith, C. Hayward, B. W. Stump, and P. Blom, (2014), "Automatic infrasound detection and location of sources in the western United States," *J. Geophys. Res. Atmos.*, vol. **119,** no. 13, pp. 7773–7798, Jul. doi: 10.1002/2013JD021084.

7 I. Hamama *et al.*, (2022), "Investigation of near-surface chemical explosions effects using seismo-acoustic and synthetic aperture radar analyses," *J. Acoust. Soc. Am.*, vol. **151**, no. 3, p. 1575, Mar. doi: 10.1121/10.0009406.

8 S. J. Arrowsmith, (2018), "False alarms and the IMS infrasound network: Understanding the factors influencing the creation of false events," *Geophys. J. Int.*, vol. **215**, no. 2, pp. 1322–1337, doi: 10.1093/GJI/GGY350.

9 A. Agrebi, A. H. Ramanantsoa, G. Rambolamanana, and E. H. Rasolomanana, (2021), "Characterisation of the Coherent Infrasound Sources Recorded by the Infrasound International Monitoring System Station I48TN in Tunisia (Mines & Quarries)," *Atmos. Clim. Sci.*, vol. **11**, no. 01, pp. 214–243, doi: 10.4236/ACS.2021.111014.

10 D. R. Christie *et al.*,(2022). "Detection of atmospheric nuclear explosions: the infrasound component of the International Monitoring System," *Kerntechnik (1987),*

vol. **66**, no. 3, pp. 96–101, 2001, Accessed: Jan. 07, [Online]. Available: http://inis.iaea.org/Search/search.aspx?orig_q=RN:32036541.

11 Y. Cansi, (1995), "An automatic seismic event processing for detection and location: The P.M.C.C. Method," *Geophys. Res. Lett.*, vol. **22**, no. 9, doi: 10.1029/95GL00468.

12 Y. Cansi and Y. Klinger, (2021) "(1) (PDF) An automated data processing method for mini-arrays," 1997. https://www.researchgate.net/publication/237698457_An_automated_data_processing_method_for_mini-arrays (accessed Apr. 17,).

13 A. Le Pichon and Y. Cansi, "Le Pichon, A. and Cansi, Y. (2003) PMCC for Infrasound Data Processing. InfraMatics, 2, 1-9. - References - Scientific Research Publishing," 2003. https://www.scirp.org/(S(czeh2tfqyw2orz553k1w0r45))/reference/ReferencesPapers.aspx?ReferenceID=1366620 (accessed Feb. 06, 2021).

14 Y. Cansi and A. Le Pichon, (2008), "Infrasound Event Detection Using the Progressive Multi-Channel Correlation Algorithm," in *Handbook of Signal Processing in Acoustics*, Springer New York, pp. 1425–1435.

15 A. M. Runco and S. Lieutenant, (2013) "Correlation Algorithm Used in Infrasound Nuclear Treaty," p. 130,.

16 O. A. Godin, D. Yu. Mikhin, and S. Y. Molchanov, (1993) "Effective sound speed approximation in the acoustics of moving media," *Izv. - Atmos. Ocean. Phys.*, vol. 29, no. 2, pp. 179–186,.

17 "Abidjan Climate, , (2022)Weather By Month, Average Temperature (Côte d'Ivoire) - Weather Spark." https://weatherspark.com (accessed Mar. 24).

18 "Max. Temperature - Abidjan - Climate Robot Côte d'Ivoire." https://www.weatheronline.co.uk/weather/maps/city?LANG=en&PLZ=_____&PLZN=_____&WMO=65578&CONT=afri&R=0&LEVEL=162&REGION=0010&LAND=IV&MOD=MOA&ART=TMX&NOREGION=1 (accessed Mar. 26, 2022).

19 J. L. Evans and A. Braun, (2012), "A climatology of subtropical cyclones in the South Atlantic," *J. Clim.*, vol. 25, no. 21, pp. 7328–7340, doi: 10.1175/JCLI-D-11-00212.1.

20 K. B. Kouassi, A. Diawara, and F. Yoroba, (2017) "Localization of Microbaroms Detected by I17CI and I11CV in IMS Data," *SnT2017*, no. T1.1-P15, p. T1.1 Infrasound and Atmospheric Dynamics, , [Online]. Available: https://ctnw.ctbto.org/ctnw/abstract/2138821 J. F. Sornein, (2000). "INFRASOUND SITE SURVEY REPORT COTE D'IVOIRE - IS 17," [Online]. Available: https://swp.ctbto.org/web/swp.